

# Technical Advance

## Immunohistochemical Localization of Feline Immunodeficiency Virus Using Native Species Antibodies

Arlin B. Rogers, Candace K. Mathiason, and Edward A. Hoover

From the Department of Microbiology, Immunology, and Pathology, Colorado State University, Fort Collins, Colorado

**Feline immunodeficiency virus (FIV) is the feline analog of human immunodeficiency virus and a small animal model of human acquired immune deficiency syndrome (AIDS). We sought to identify early *in vivo* target cells in cats infected with clade B or C FIV. In tissues, however, neither mouse monoclonal nor rabbit polyclonal antibodies suitably detected FIV because of either insensitivity or lack of specificity. We therefore developed an immunohistochemical protocol using high-antibody-titer serum from cats chronically infected with FIV<sub>Petaluma</sub>. Native species anti-FIV antibodies were labeled with biotinylated protein A before placement on tissues, and downstream signal was tyramide-amplified. This method revealed many productively infected cells in bone marrow, lymph node, thymus, mucosal-associated lymphoid tissue, and spleen, but few such cells in liver and none in kidney or brain. Concurrent labeling for virus and cell phenotype revealed that antigen-bearing populations were primarily T lymphocytes but included macrophages and dendritic cells. Our results demonstrate that FIV: 1) expands rapidly in T cells, 2) targets long-lived reservoir populations, and 3) is replicatively quiescent in brain at 3 weeks after infection. Use of native species antibodies for immunohistochemical detection of infectious antigens has application to other settings in which xenotypic (eg, mouse and rabbit) antibody sources are inadequate or unavailable. (Am J Pathol 2002, 161:1143-1151)**

Elucidating host-virus interactions *in vivo* depends in large part on the localization of virus to specific cells in tissues. *In situ* identification of human immunodeficiency virus (HIV)-1 RNA in human lymphoid tissues demonstrates that viral replication continues even with declining or unde-

tectable viral loads in plasma.<sup>1-4</sup> However, tissue-based studies of early HIV pathogenesis are dependent on access to limited biopsy or autopsy materials. For that reason, animal models can be used to help characterize early lentiviral disease progression *in vivo*.

Feline immunodeficiency virus (FIV) infection in cats causes disease virtually indistinguishable from that caused by HIV-1 in humans and simian immunodeficiency virus (SIV) in Asian macaques.<sup>5,6</sup> The anatomical distribution of FIV is similar to that of HIV-1 and SIV and includes mucosal interfaces, lymphoid organs, sites of hematopoiesis, circulating mononuclear cells, and the central nervous system.<sup>7-13</sup> Proven *in vitro* FIV cell targets include T lymphocytes,<sup>14,15</sup> monocytes/macrophages,<sup>12,16</sup> dendritic cells,<sup>10,17-20</sup> and central nervous system astrocytes, and macrophages.<sup>21,22</sup>

Characterization of FIV pathogenesis *in vivo* has been limited by a shortage of reagents for identification of cell phenotypes in feline tissue sections, and by the small number of described assays for detecting virus *in situ*. FIV is most often revealed in tissue sections by *in situ* RNA hybridization.<sup>10,17,18,23-28</sup> However, tissue digestion steps required for *in situ* RNA hybridization often destroy protease-sensitive cell-specific antigens, limiting the number of markers available to identify the cells infected. Moreover, the special precautions required to prevent target and probe degradation by RNases and the relatively high cost of developing or purchasing FIV RNA probes have limited the application of this technique. Identification of FIV-specific proteins by immunohistochemistry obviates the need for protease digestion steps and RNase-free protocols. However, few monoclonal antibodies proven to sensitively and specifically bind FIV in tissue sections are

---

Supported by the National Institutes of Health (grants HD34338 to E. A. H. and AI01420 to A. B. R.).

Accepted for publication June 18, 2002.

Current address of A. B. R.: Division of Comparative Medicine, Massachusetts Institute of Technology, Cambridge, Massachusetts.

Address reprint requests to Edward A. Hoover, D.V.M., Ph.D., Department of Microbiology, Immunology, and Pathology, Colorado State University, Fort Collins, Colorado 80523-1674. E-mail: ehoover@lamar.colostate.edu

available. Additionally, because monoclonal antibodies only bind a single epitope, high virus copy number may be required for detection. Thus, there are few reports of FIV identification in tissue sections by immunostaining.<sup>19,27</sup>

In this report we describe a modified immunohistochemical assay that complemented other *in situ* methodologies for the detection and quantitation of virus in tissues from cats infected with clade B or clade C FIV.<sup>29,30</sup> FIV-B-2542 and FIV-C<sub>PaddyGammer</sub> (FIV-C-Pgmr) replicate to high titer during acute-phase infection and can be transmitted mucosally.<sup>10,26,31–33</sup> The results described in this report contribute further insights into the cell targets and tissue replication kinetics of FIV during acute infection.

## Materials and Methods

### Animals and Tissue Processing

Two groups (five cats per group) of 8-week-old cats from a specific pathogen-free breeding colony maintained at Colorado State University (Fort Collins, CO) were inoculated intravenously with 100 tissue culture infectious doses (TCID) of acute-phase plasma pools of FIV.<sup>34</sup> Cats were inoculated with FIV-B-2542<sup>35</sup> or FIV-C-Pgmr.<sup>36</sup> The cats were observed daily for signs of illness after virus inoculation. Three weeks after inoculation, blood was collected and the animals were euthanized. Tissues collected at necropsy included brain, peripheral and internal lymph nodes, thymus, liver, spleen, small and large intestine, pancreas, kidney, and bone marrow. Blood and tissues from an age-matched uninfected specific pathogen-free cat were used as negative controls. Tissues were preserved in a variety of fixatives including 10% neutral buffered formalin, absolute ethanol, and Histochoice-MB (Amresco, Solon, OH). Tissues were fixed overnight and processed the following morning into paraffin-embedded blocks by a short-run method that avoided the use of formalin and that minimized immersion time in liquid paraffin (Colorado State University Histology Laboratory, Fort Collins, CO). Routine 5- $\mu$ m paraffin sections were placed on silanized slides without heat treatment and allowed to air dry at least 1 day before staining.

### Polymerase Chain Reaction and TCID Assays

Purified blood mononuclear cells from FIV-infected cats were assayed for FIV by nested DNA PCR as described elsewhere<sup>9</sup> except that first round primers were modified to increase specificity. The updated first round primers were gag 129 (5'-CGTAACTACAGGACGAGAACCTG-3') and gag 802 (5'-CCAACTTCCCAATGCTTCAAG-3'; Sigma-Genosys, The Woodlands, TX). Semiquantitative plasma viral RNA loads were determined using a previously described method.<sup>30</sup> TCID determination of virus in plasma and blood mononuclear cells was assessed by serial dilution and co-cultivation with primary naïve feline blood mononuclear cells as previously described.<sup>30</sup>

### Chromogenic Immunohistochemistry

Tissue sections on silanized glass slides were deparaffinized with brief heat treatment and rehydrated through xylene and graded alcohols to water, and then washed in TENT solution (0.05 mol/L Tris, pH 7.4, 1 mmol/L ethylenediaminetetraacetic acid (EDTA) sodium, 0.15 mol/L NaCl, 0.05% Tween). Formalin-fixed sections were subjected to 10 minutes of microwave antigen retrieval in citrate Antigen Unmasking Solution (Vector Laboratories, Burlingame, CA) followed by slow cooling at room temperature for 20 minutes. Endogenous peroxidases were quenched with 3% H<sub>2</sub>O<sub>2</sub> in phosphate-buffered saline (PBS, pH 7.4). Sections were blocked in 1% each naïve goat and cat serum in TNB blocking buffer (TSA System; NEN, Boston, MA). A second block was performed with 1  $\mu$ g/ml of unconjugated protein A (Sigma Chemical Co., St. Louis, MO) in TNB. While the tissue sections were being blocked, equal parts high titer antibody-positive plasma from one of two cats chronically infected with FIV-A-Petaluma<sup>35,37</sup> and 1 mg/ml of stock biotin-conjugated protein A (Sigma) were diluted 1:100 in TNB and allowed to bind at room temperature in solution. After 20 minutes of protein A-biotin binding to antibody at the Fc fragment, the solution was further diluted as determined empirically for a given collection of plasma. Final dilutions typically ranged from 1:1000 to 1:10,000. Tissue sections were washed and then incubated with the protein A-biotin-labeled antibody solution in a humidified chamber at 37°C for 2 hours. Slides were washed and biotin was labeled with Extravidin-peroxidase (Sigma) followed by tyramide amplification using the TSA Biotin System (NEN). Positive signal was detected with 3,3'-diaminobenzidine tetrahydrochloride, Vector VIP, or Nova Red chromogens (Vector Laboratories) and counterstained with Gill's hematoxylin, methyl green (Vector), or 0.5% Evan's blue dye (Sigma). Sections were dehydrated through graded alcohols to xylene, mounted with Cytoseal XYL (Stephens Scientific, Kalamazoo, MI), and routinely coverslipped. Equivalent specimens from a sham-inoculated specific pathogen-free cat were included in each run as negative controls.

### Morphometric Analysis

Digital images of immunostained tissues were captured using the 3-CCD 1140  $\times$  1520 detail CoolSNAP camera and software system (Roper Scientific GmbH, Bergkirchen, Germany) and were analyzed with MetaMorph software (Universal Imaging Corp., West Chester, PA). Using a stage micrometer, field area through the  $\times$ 20 objective was determined to be 0.13 mm<sup>2</sup>. Positively stained cells were enumerated using thresholding (color calibration) and cell counting functions. Average pixel area per positive cell was determined by summing the area of chromogen stain in 50 individual FIV<sup>+</sup> cells and dividing the total by 50. Positive cell counts were determined by measuring the total pixel area of chromogen within the field and dividing the total positive pixel area by the average value per positively stained cell for that re-

gion. Ten fields per tissue were counted. Field cell counts were logged into an Excel spreadsheet (Microsoft Corp., Redmond, WA) from which mean values and standard deviations were calculated. Because preliminary evaluation demonstrated no significant differences between the FIV-B-2542 and FIV-C-Pgmr source tissues, reported values are for the FIV-infected cats as a group. To estimate the number of FIV<sup>+</sup> cells per gram of tissue, we made the assumption that the examined field was representative of the compartment as a whole. We then determined the number of FIV<sup>+</sup> cells per cm<sup>2</sup> tissue using the formula:

$$\frac{\text{FivPosCells}}{0.13\text{mm}^2} * \frac{100\text{mm}^2}{\text{cm}^2} = \frac{\text{FivPosCells}}{\text{cm}^2}$$

Assuming that 1 g of tissue = ~1 cm<sup>3</sup>, we used the following formula to estimate the number of FIV<sup>+</sup> cells per g tissue:

$$\sqrt{\frac{\text{FivPosCells}^3}{\text{cm}^2}} = \frac{\text{FivPosCells}}{\text{g}}$$

### RNA in Situ Hybridization

FIV RNA was demonstrated in formalin-fixed tissue sections using a previously described *in situ* hybridization protocol.<sup>10</sup>

### Fluorescence Immunohistochemistry

For fluorescence immunohistochemistry, we amplified FIV signal with Cy3-conjugated tyramide (NEN). Cell phenotype antibodies were labeled with species-appropriate fluorescein isothiocyanate-conjugated secondary antibodies (Sigma). T cells were labeled with polyclonal rabbit anti-CD3 antibody (Sigma). Monocytes bearing lipopolysaccharide receptors were detected with anti-CD14 (DAKO, Carpinteria, CA) or Alexa 488-conjugated lipopolysaccharide (Molecular Probes, Eugene, OR). Four antibodies were used to identify subsets of tissue macrophages: AM-3K (a gift from M. Takeya, Osaka Prefecture University, Sakai, Japan),<sup>38-40</sup> FeMy, which recognizes a feline myeloid cell antigen,<sup>41</sup> Mac 387, which labels a subset of macrophages and polymorphonuclear cells (Serotec), and anti-CD 74 (Sigma), a histiocyte marker. Dendritic cells were labeled with anti-follicular dendritic cell monoclonal CNA.42 (DAKO), anti-fascin (anti-p55, DAKO), or rabbit polyclonal anti-S-100 (Serotec). Mesenchymal cells (including leukocytes) were differentiated from epithelial cells by labeling for the intermediate filaments vimentin and cytokeratin, respectively (Serotec). Unless otherwise stated, all of the cell phenotype markers listed above are mouse anti-human monoclonal antibodies.

After fluorescent antibody labeling, cell nuclei were stained with 1 μg/ml of 4',6-diamidino-2-phenylindole dihydrochloride (DAPI, Sigma) for 1 minute. Sections were allowed to partially air dry and were mounted with Vectashield (Vector). Digital images were captured using the CoolSnap system on an Olympus BX60 microscope

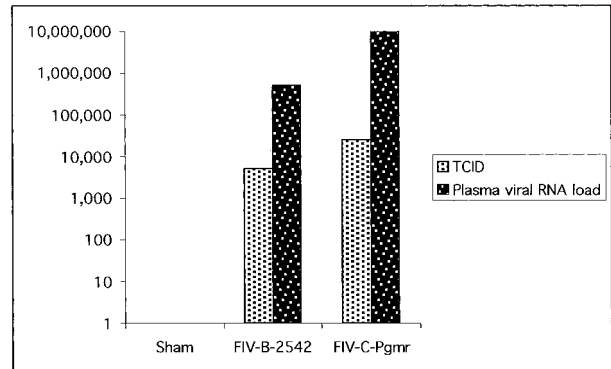


**Figure 1.** Mean FIV blood mononuclear cell supernatant tissue culture infectious doses (TCID/ml) and plasma viral RNA loads (copies/ml) 3 weeks after inoculation in cats infected with FIV-B-2542 or FIV-C-Pgmr.

(Olympus America, Lake Success, NY). Serial images of multistained fluorescent sections were overlaid using Adobe Photoshop software (Adobe Systems, San Jose, CA) on a Power Macintosh G4 computer (Apple Computer, Cupertino, CA).

## Results

### FIV Acute Infection Kinetics

All cats inoculated with FIV were positive by DNA polymerase chain reaction on isolated blood mononuclear cells collected 3 weeks after inoculation at the time of necropsy (not shown). Plasma viral RNA loads ranged from 10<sup>5</sup> to 10<sup>6</sup> copies/ml in cats inoculated with FIV-B-2542, and 10<sup>6</sup> to 10<sup>8</sup> copies/ml in cats inoculated with FIV-C-Pgmr (Figure 1). Pooled plasma-inoculated supernatant TCID means were 5.1 × 10<sup>3</sup> TCID/ml for the FIV-B-2542 group and 2.5 × 10<sup>4</sup> TCID/ml for the FIV-C-Pgmr cohort (Figure 1). Blood mononuclear cells and plasma from the sham-inoculated cat were negative for FIV by polymerase chain reaction and co-culture.

### Chromogenic Immunohistochemistry

FIV antigens were detected in tissues of all acutely infected cats (Figure 2a). No labeling occurred in FIV<sup>+</sup> tissues when antiserum from FIV-naïve cats was used as the primary antibody source, nor was there labeling of tissues from the sham-inoculated cat regardless of antiserum source (Figure 2b). For detecting FIV proteins, ethanol- and Histochoice-fixed tissues proved superior to antigen-retrieved formalin-fixed specimens (not shown). No FIV detection was observed in formalin-fixed tissues without microwave antigen retrieval.

In lymph nodes, most FIV<sup>+</sup> cells were found in germinal centers and in paracortical regions (Figure 2a). In germinal centers, FIV was detected in or on the surface of large stellate cells with arborizing extensions, suggestive of antigen trapping along a follicular dendritic cell network. Within the thymus, FIV<sup>+</sup> immature thymocytes in the peripheral cortex outnumbered infected mature thymocytes in the medulla, and antigen detection was espe-

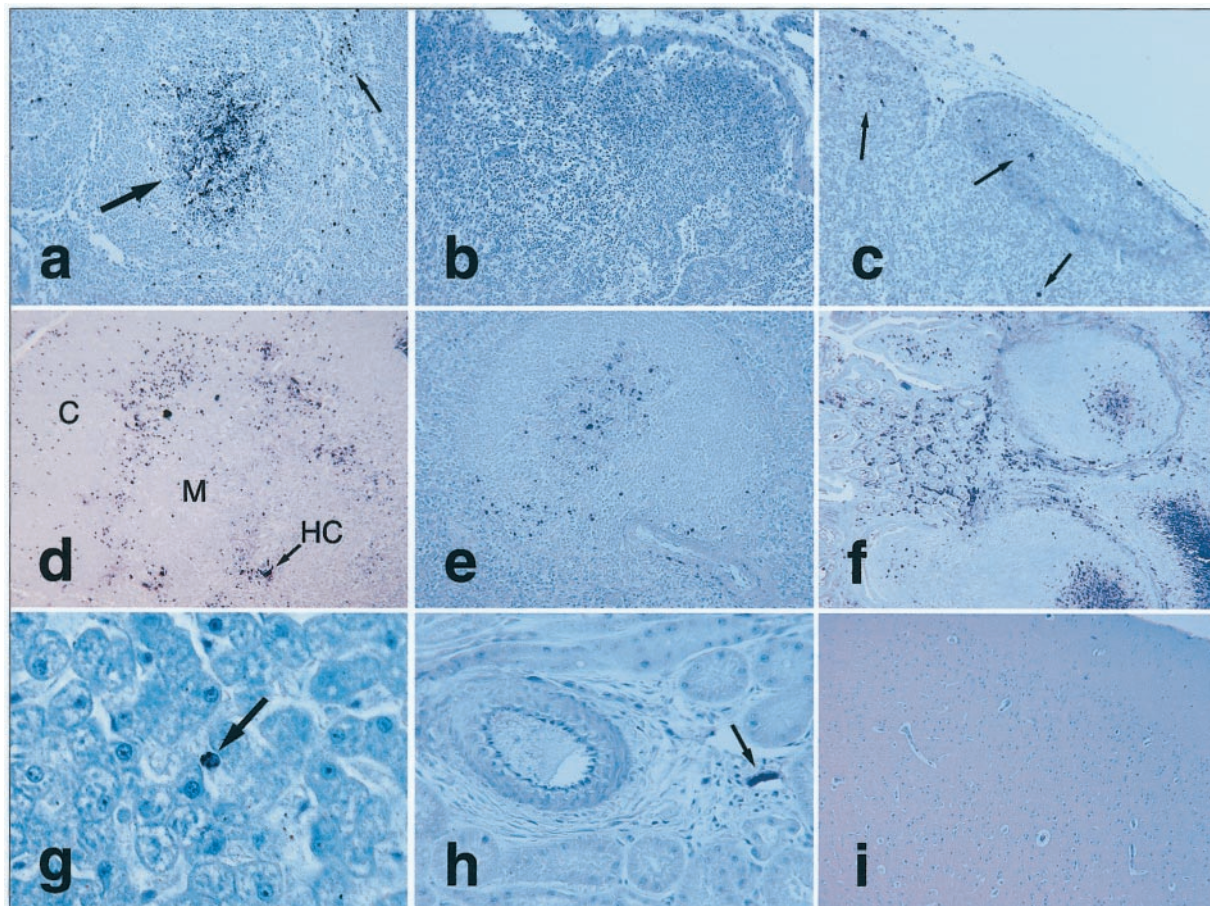


**Figure 2.** FIV chromogenic immunohistochemistry. **a:** FIV antigen<sup>+</sup> cells in lymph node germinal center (large arrow) and paracortical cells (small arrow). **b:** No FIV antigens in sham-inoculated control cat lymph node. **c:** Scattered labeled cells (arrows) by RNA *in situ* hybridization in lymph node from FIV<sup>+</sup> cat. FIV immunohistochemistry on tissues from FIV<sup>+</sup> cat including: thymic lobule with clustering of antigen<sup>+</sup> cells along junction between cortex (C) and medulla (M), with additional antigen localization in or near Hassal's corpuscle (HC) (**d**, arrow); viral antigen expression in splenic periarteriolar lymphatic sheaths (**e**); abundant FIV antigen in ileal lamina propria leukocytes and mucosal-associated lymphoid tissue (Peyer's patch) germinal centers (**f**); one antigen<sup>+</sup> mononuclear cell (arrow) in lumen or lining hepatic sinusoid (**g**); apparently cell-free virus lining endothelial surface of small venule in kidney (arrow), but not in renal tubules or larger artery (at left; **h**); and brain with no detectable viral antigens (**i**). Original magnifications:  $\times 200$  (**a**, **c**, and **e**),  $\times 100$  (**b** and **d**),  $\times 240$  (**f**),  $\times 600$  (**g**),  $\times 400$  (**h**), and  $\times 40$  (**i**).

cially prominent at the corticomedullary junction (Figure 2d). Most FIV expression in the thymic medulla was near or within Hassal's corpuscles. Within the spleen, most FIV<sup>+</sup> cells were located in hyperplastic periarteriolar lymphatic sheaths (Figure 2e). Periarteriolar lymphatic sheath hyperplasia, with occasional follicle formation, was common in FIV-infected cat tissues but not in naïve controls. Few FIV antigen<sup>+</sup> cells were identified in red pulp. There were abundant FIV<sup>+</sup> mononuclear cells in the lamina propria of all intestinal sections examined (Figure 2f). Indeed, intestinal sections proved to be one of the most consistent tissue sources for detecting FIV. Mucosal-associated lymphoid tissue in the ileum (Peyer's patches) demonstrated reactive and hyperplastic changes in FIV-infected cats, with abundant germinal center FIV antigens.

Liver contained scattered intra- or perisinusoidal FIV<sup>+</sup> cells morphologically consistent with Kupffer cells or circulating mononuclear cells (Figure 2g). FIV antigens were not demonstrated in resident cells of nonlymphoid organs such as pancreas and kidney. However, non-cell-associated staining of endothelial surfaces of small ves-

sels, but not large vessels, was observed in nonlymphoid as well as lymphoid organs (Figure 2h). Although many FIV isolates, including FIV-B-2542, have a known tropism for the central nervous system,<sup>9,22,42</sup> we identified no FIV antigens in the brains of these animals at our collection point 3 weeks after inoculation (Figure 2i).

### Morphometric Analysis

As expected, lymphoid and hematopoietic organs exhibited high concentrations of FIV, with calculated values  $>1$  million antigen<sup>+</sup> cells per gram of tissue in lymph node, thymus, and bone marrow (Table 1). Intestinal sections contained a high concentration of FIV<sup>+</sup> leukocytes in the lamina propria and submucosa. Indeed, when only those layers were considered, FIV<sup>+</sup> cell concentrations were equivalent to those in lymphoid compartments (Table 1). Spleen had a lower overall tissue virus burden, because most antigen<sup>+</sup> cells were concentrated in periarteriolar lymphatic sheath. Only a few perisinusoidal mononuclear cells contained FIV antigen in liver, and no cell-assoc-

**Table 1.** Concentration of Viral Antigen<sup>+</sup> Cells in Tissues from Cats Acutely Infected with FIV

Tissue	FIV <sup>+</sup> cells/×20 field*	FIV <sup>+</sup> cells/g tissue
Brain	0	0
Thymus	15.3	1,278,713
Lymph node	18.5	1,700,175
Liver	0.6	9,930
Spleen	8.0	483,472
Intestine <sup>†</sup>	12.1	899,320
Kidney	0	0
Bone marrow	14.3	1,155,421

\*Mean for all FIV<sup>+</sup> cats; non-cell-associated virus excluded; ×20 objective field = 0.13 mm<sup>2</sup>.

<sup>†</sup>Mucosa and submucosa only; all FIV<sup>+</sup> cells were morphologically consistent with leukocytes.

ated virus was detected in brain, kidney, or pancreas, although cell-free virus (not quantitated) lined the endothelial surface of small vessels in some sections of the latter two tissue types.

### RNA in Situ Hybridization

We detected FIV<sup>+</sup> cells by RNA *in situ* hybridization in many of the same tissues positive by immunohistochemistry (Figure 2c). Tissues from the sham-inoculated cat were negative. However, qualitative comparison of RNA *in situ* hybridization versus immunohistochemistry revealed that in our hands immunohistochemistry was superior for retention of tissue architecture and was equivalent or superior in sensitivity with the same high specificity.

### Fluorescence Immunohistochemistry

For three-color fluorescence immunohistochemistry we labeled FIV red with Cy3, cell phenotype markers green with fluorescein, and nuclei blue with DAPI (Figure 3a). Most phenotypically identified cells containing detectable FIV antigens were CD3<sup>+</sup> T cells (Figure 3b). In most lymphoid tissues, ~10 to 15% of FIV<sup>+</sup> were macrophages detected with monoclonal antibody AM-3K (Figure 3c). AM-3K labeled many more tissue macrophages than did the other histiocyte markers we used including Mac 387, FeMy, and CD74. Monocyte/macrophages bearing lipopolysaccharide receptors, as determined by labeling with anti-CD14 antibody or Alexa 488-conjugated lipopolysaccharide, very rarely contained detectable FIV antigens. Five to 10% of FIV<sup>+</sup> cells in lymphoid organs were S-100<sup>+</sup> (Figure 3d). These were probably dendritic cells, although S-100 antigen is also found in cells of the nervous system and in melanocytes.<sup>43</sup> Thymic medullary dendritic cells labeled with antibody CNA.42 (DAKO). CNA.42 is an antibody derived from a human follicular dendritic cell antigen. Feline thymic CNA.42<sup>+</sup> dendritic cells rarely contained detectable FIV antigens. Moreover, in feline lymph nodes CNA.42 recognized parafollicular interdigitating dendritic cells but not germinal center follicular dendritic cells. In all tissues FIV antigens were rarely if ever detected in or on CNA.42<sup>+</sup> cells (Figure 2h). Likewise, FIV rarely co-localized with the interdigitating follicular cell marker fascin (p55; DAKO) in

lymph nodes. FIV antigens were detected in large MHCII<sup>hi</sup> antigen-presenting cells in lymph node germinal centers, which likely included follicular dendritic cells and macrophages.

Some cytokeratin<sup>+</sup> cells in the deep thymic medulla co-localized with FIV antigens (Figure 3e). In all other tissues only vimentin<sup>+</sup> cells and not cytokeratin<sup>+</sup> cells contained FIV antigens. In the thymus, many phenotypically unidentified FIV<sup>+</sup> cells in the cortex were morphologically consistent with immature thymocytes (Figure 3f). CD45R/B220<sup>+</sup> B cell infiltrates occasionally formed pseudofollicles in the thymuses of FIV-infected cats (Figure 3g), but were absent from the sham-inoculated cat. B cells in all tissues contained no detectable FIV antigens. In sections of intestine we identified FIV<sup>+</sup> CD3<sup>+</sup> T cells and S-100<sup>+</sup> dendritic cells, but many FIV<sup>+</sup> leukocytes were not labeled by any of our phenotypic markers. Bone marrow was a rich source of phenotypically unidentified FIV antigen<sup>+</sup> cells. These were likely immature leukocyte progenitors.

### Discussion

In this report we describe a modified immunohistochemical protocol for the localization of FIV in feline tissues. We developed the protocol using native species antibodies only after exhausting more traditional approaches. Although murine monoclonal antibodies can detect by immunocytochemistry FIV in stimulated cells from primary culture with very high viral antigen levels,<sup>12</sup> we found no murine monoclonal antibody or combination of such antibodies sufficiently sensitive to detect FIV in tissue sections (not shown). In hopes of increasing sensitivity, we generated rabbit anti-FIV polyclonal antisera, but ultimately were forced to abandon this source as well because of high background staining (not shown), possibly in part because of the use of complete and incomplete Freund's adjuvant. For the native species antibody assay described in this report, we labeled feline antibodies with biotinylated protein A, a staphylococcal product that binds at the Fc fragment, to leave the antigen recognition site free for epitope binding. Tissues were blocked with unlabeled protein A before application of the labeled antibodies. Streptococcal protein G also binds Fc fragments, but has a species affinity different from protein A, and does not bind feline antibodies.

Our immunohistochemistry protocol held two advantages over RNA *in situ* hybridization. First, for RNA *in situ* hybridization protease digestion had to be optimized for each tissue, a cumbersome enterprise, and there was always reduction in morphological detail. Second, by using undigested nonformalin-fixed tissues in immunohistochemistry, a much broader array of cell phenotype markers was available for co-localization studies. In our hands RNA *in situ* hybridization was no more sensitive than immunohistochemistry, although had we used a radiolabeled probe we might have increased hybridization sensitivity.<sup>1</sup>

Our modified immunostaining protocol permitted us to broadly survey the tissue distribution and cell types tar-

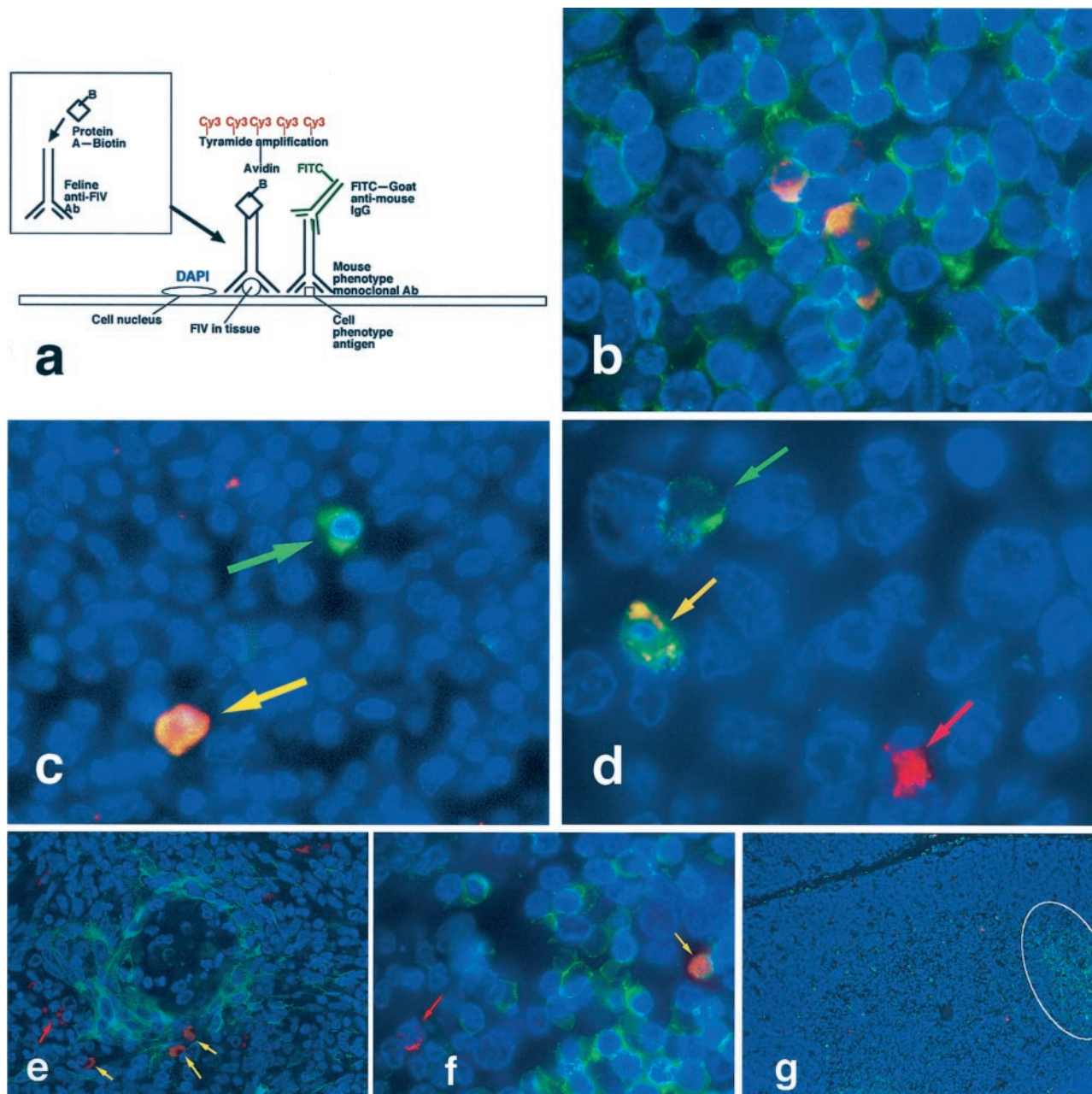


**Figure 3.** Fluorescence immunohistochemistry. **a:** Diagram of three-color immunofluorescence assay demonstrating prelabeling of heterologous antiserum with biotin-protein A followed by tissue binding and Cy3-tyramide amplification for red labeling of FIV, fluorescein isothiocyanate-conjugated secondary antibodies for green labeling of cell phenotype antibodies, and DAPI counterstaining for blue labeling of nuclear chromatin. **b:** FIV antigens co-localized with CD3<sup>+</sup> T cells in lymph node paracortex. **c:** An FIV<sup>+</sup> AM-3K-labeled macrophage (**yellow arrow**) and a macrophage without FIV antigens (**green arrow**) in lymph node medulla. **d:** S-100<sup>+</sup> dendritic cells with (**yellow arrow**) and without (**green arrow**) FIV antigens in lymph node follicle; also present is a FIV<sup>+</sup> S-100<sup>-</sup> cell (**red arrow**). **e:** A few cytokeratin<sup>+</sup> thymic epithelial cells (**yellow arrows**) as well as cytokeratin<sup>-</sup> FIV<sup>+</sup> cells (**red arrow**) that are probably mature thymocytes in medulla. **f:** FIV antigens in both CD3<sup>+</sup> (**yellow arrow**) and CD3<sup>-</sup> (**red arrow**) cortical thymocytes. **g:** CD45R/B220<sup>+</sup> B cell infiltrates, occasionally forming pseudofollicles (**outlined**) in thymus of FIV-infected cat. Original magnifications:  $\times 1000$  (**b** and **d**),  $\times 600$  (**c** and **f**),  $\times 400$  (**f**),  $\times 200$  (**e**), and  $\times 100$  (**g**).

geted by FIV. The drawbacks of using native host species antisera as polyclonal antibody source include: 1) the need for empirical titration of every plasma collection because of titer variation between individuals and within the same individual over time, 2) the presence of potentially confounding nonspecific antibodies, and 3) difficulty in assay standardization between users and laboratories. However, we found that with optimization and vigorous attention to blocking and controls, our assay

was repeatable, sensitive, and specific within our specific pathogen-free experimental setting. Apart from the serum titer of the primary antibody source, the greatest determinant of success in our histological studies was choice of tissue fixatives. Although we could detect some FIV antigens in formalin-fixed tissues subjected to microwave antigen retrieval, we found that sensitivity in such specimens was markedly lower than that seen in the same tissues fixed with the precipitating agent ethanol or pro-

prietary non-cross-linking preservative Histochoice. Thus, our study agrees with others that non-cross-linking fixatives may suitably conserve antigenic integrity for immunohistochemistry while preserving a degree of tissue morphological integrity superior to that usually seen in frozen sections.<sup>44</sup>

As expected, lymphoid organs including lymph node, thymus, and spleen were important sites of FIV propagation. Bone marrow also exhibited a high *in situ* viral burden by 3 weeks after infection. Somewhat surprising to us was the marked tropism of virus for intestinal leukocytes and gut-associated lymphoid tissue, although intestinal localization of virus is well known in macaques infected with SIV and SIV/HIV.<sup>45,46</sup> Because the cats were inoculated intravenously, intestinal leukocytes presumably acquired virus in the circulation or within a lymphoid compartment before trafficking to enteric mucosa. Local cell-to-cell transmission may have occurred once virus reached the intestinal compartment. In both lymphoid and nonlymphoid tissues except brain, we detected apparently cell-free virus lining the endothelial surface of small vessels but not large vessels. We did not determine whether selective detection of cell-free virus in small vessels represented a biological or methodological phenomenon.

In SIV-infected macaques, viral RNA has been detected by *in situ* hybridization in CD14<sup>+</sup> perivascular macrophages in the brain at 2 weeks after inoculation.<sup>47</sup> We did not detect FIV antigens in any brain sections collected 3 weeks after inoculation from these cats. Moreover, FIV antigen<sup>+</sup> CD14<sup>+</sup> monocytes/macrophages were rare in any tissue by our methods. Future studies may help determine whether there is an actual difference in central nervous system viral expression at different time points during acute infection, whether there is a pathogenetic difference between the FIV isolates we studied and neurotropic SIV, or whether the discrepancy was the result of methodological differences. Apart from reactive lymphoid hyperplasia in multiple tissues, the only morphological lesion we observed in the FIV-infected cats was infiltration of the thymus with B lymphocytes, which sometimes formed pseudofollicles. Other investigators have observed thymic B cell infiltrates in animals infected with FIV<sup>24,48</sup> and SIV.<sup>49</sup> No B cells in our study contained detectable FIV.

The virulent FIV isolates we used in this study resulted in a large number of FIV<sup>+</sup> cells per gram of lymphoid tissue as determined by morphometric analysis. These values are in agreement with equivalent studies demonstrating high lymphoid tissue viral RNA burdens in people during acute-phase HIV-1 infection.<sup>4</sup> As in previous studies from our laboratory, FIV-B-2542 and FIV-C-Pgmr reached high plasma viral RNA and blood mononuclear cell proviral titers.<sup>10,31,50,51</sup> Plasma and mononuclear cells from infected cats readily infected naïve feline blood mononuclear cells in culture and resulted in high TCIDs in the supernatants. Thus, *in vitro* data corroborated our finding of widespread and productive infection *in vivo*.

FIV-B-2542 and FIV-C-Pgmr infected the same range of cells known to be targeted by HIV-1 and SIV, including but not limited to T lymphocytes, macrophages, and den-

dritic cells.<sup>52,53</sup> In this group of cats in the acute-phase of infection, ~70 to 85% of phenotypically identified cells with detectable FIV antigen were T cells. The remaining FIV antigen<sup>+</sup> phenotypically identified cells were macrophages, follicular dendritic cells, and occasional thymic epithelial cells. We were unable to identify the phenotype of many FIV<sup>+</sup> cells, particularly in the intestine, thymic cortex, and bone marrow. Unidentified FIV<sup>+</sup> leukocytes in intestine may have included CD3<sup>-</sup> intraepithelial lymphocytes, natural killer cells, and/or macrophage subsets not recognized by our histiocytic markers. In the thymic cortex and bone marrow, the unidentified FIV<sup>+</sup> cells probably included CD3<sup>-</sup> cortical thymocytes and leukocyte progenitors, respectively.

Our finding of acute-phase T lymphocyte tropism is in agreement with other studies that demonstrate that lentiviral expansion occurs in T cells from the earliest phases of infection onward.<sup>54</sup> Previous studies with FIV-C-Pgmr demonstrated early thymic tropism after transmucosal inoculation.<sup>10</sup> Transmucosal infection by HIV-1 and SIV may involve T cells directly at the site of exposure.<sup>45,55,56</sup> As early as day 2 days after vaginal inoculation, simian/human immunodeficiency virus (SHIV)<sup>+</sup> cells are detected in cortical parafollicular cells of lymph nodes in pig-tailed macaques.<sup>57</sup> Macaques vaginally inoculated with SIV<sub>mac</sub>251 demonstrate infection of intraepithelial dendritic cells (Langerhans cells) within 1 hour, but within 24 hours the majority of cells infected are T cells, both at the site of inoculation and in regional lymph nodes.<sup>58</sup> Thus, regardless of the cell types first targeted by lentiviruses, it seems clear that CD4<sup>+</sup> T cells rapidly constitute the majority of cells productively infected after initial exposure.<sup>59</sup>

In summary, we describe a modified immunohistochemical assay for detecting and quantitating FIV *in vivo*. Most phenotypically identified FIV antigen<sup>+</sup> cells were T cells, but viral proteins also co-localized with macrophages, dendritic cells, and occasional thymic epithelial cells. Further work is needed to classify the full range of cells infected by FIV *in vivo*. Our studies reinforce the value of collecting tissues in multiple fixatives, and corroborate the work of others demonstrating that non-cross-linking fixatives may provide an attractive alternative to frozen sections for many *in situ* immunoassays.<sup>44</sup> Continued refinement of methods for detecting FIV in tissues will enhance our understanding of lentiviral pathogenesis, which may point to new targets for the prevention and intervention of HIV and acquired immune deficiency syndrome.

### Acknowledgments

We thank Andrea Lauerma for animal care, Jen Keane for help with sample collection, and Kevin Keane for assistance with morphometric analysis.

### References

1. Haase AT, Henry K, Zupancic M, Sedgewick G, Faust RA, Melroe H, Cavert W, Gebhard K, Staskus K, Zhang ZQ, Dailey PJ, Balfour Jr HH,

- Erice A, Perelson AS: Quantitative image analysis of HIV-1 infection in lymphoid tissue. *Science* 1996, 274:985–989
2. Zhang ZQ, Notermans DW, Sedgewick G, Cavert W, Wietgreffe S, Zupancic M, Gebhard K, Henry K, Boies L, Chen Z, Jenkins M, Mills R, McDade H, Goodwin C, Schuwirth CM, Danner SA, Haase AT: Kinetics of CD4+ T cell repopulation of lymphoid tissues after treatment of HIV-1 infection. *Proc Natl Acad Sci USA* 1998, 95:1154–1159
  3. Embretson J, Zupancic M, Ribas JL, Burke A, Racz P, Tenner-Racz K, Haase AT: Massive covert infection of helper T lymphocytes and macrophages by HIV during the incubation period of AIDS. *Nature* 1993, 362:359–362
  4. Schacker T, Little S, Connick E, Gebhard-Mitchell K, Zhang ZQ, Krieger J, Pryor J, Havlir D, Wong JK, Richman D, Corey L, Haase AT: Rapid accumulation of human immunodeficiency virus (HIV) in lymphatic tissue reservoirs during acute and early HIV infection: implications for timing of antiretroviral therapy. *J Infect Dis* 2000, 181:354–357
  5. Hartmann K: Feline immunodeficiency virus infection: an overview. *Vet J* 1998, 155:123–137
  6. Geretti AM: Simian immunodeficiency virus as a model of human HIV disease. *Rev Med Virol* 1999, 9:57–67
  7. Brown PJ, Hopper CD, Harbour DA: Pathological features of lymphoid tissues in cats with natural feline immunodeficiency virus infection. *J Comp Pathol* 1991, 104:345–355
  8. Callanan JJ, Thompson H, Toth SR, O'Neil B, Lawrence CE, Willett B, Jarrett O: Clinical and pathological findings in feline immunodeficiency virus experimental infection. *Vet Immunol Immunopathol* 1992, 35:3–13
  9. Rogers AB, Hoover EA: Maternal-fetal feline immunodeficiency virus transmission: timing and tissue tropisms. *J Infect Dis* 1998, 178:960–967
  10. Obert LA, Hoover EA: Relationship of lymphoid lesions to disease course in mucosal feline immunodeficiency virus type C infection. *Vet Pathol* 2000, 37:386–401
  11. Hein A, Martin JP, Koehren F, Bingen A, Dorries R: In vivo infection of ramified microglia from adult cat central nervous system by feline immunodeficiency virus. *Virology* 2000, 268:420–429
  12. Dow SW, Mathiason CK, Hoover EA: In vivo monocyte tropism of pathogenic feline immunodeficiency viruses. *J Virol* 1999, 73:6852–6861
  13. Macchi S, Maggi F, Di Iorio C, Poli A, Bendinelli M, Pistello M: Detection of feline immunodeficiency proviral sequences in lymphoid tissues and the central nervous system by in situ gene amplification. *J Virol Methods* 1998, 73:109–119
  14. Lerner DL, Elder JH: Expanded host cell tropism and cytopathic properties of feline immunodeficiency virus strain PPR subsequent to passage through interleukin-2-independent T cells. *J Virol* 2000, 74:1854–1863
  15. Chen ZW, Shen Y, Davis IC, Shen L, Letvin NL, Fultz PN: Down-regulation of macaque gamma delta + T cells in lymphoid compartments after rectal infection with SIVsmmPBj14. *J Med Primatol* 2000, 29:143–147
  16. Dean GA, Himathongkham S, Sparger EE: Differential cell tropism of feline immunodeficiency virus molecular clones in vivo. *J Virol* 1999, 73:2596–2603
  17. Bach JM, Hurtrel M, Chakrabarti L, Ganiere JP, Montagnier L, Hurtrel B: Early stages of feline immunodeficiency virus infection in lymph nodes and spleen. *AIDS Res Hum Retroviruses* 1994, 10:1731–1738
  18. Hurtrel B, Chakrabarti L, Hurtrel M, Bach JM, Ganiere JP, Montagnier L: Early events in lymph nodes during infection with SIV and FIV. *Res Virol* 1994, 145:221–227
  19. Toyosaki T, Miyazawa T, Furuya T, Tomonaga K, Shin YS, Okita M, Kawaguchi Y, Kai C, Mori S, Mikami T: Localization of the viral antigen of feline immunodeficiency virus in the lymph nodes of cats at the early stage of infection. *Arch Virol* 1993, 131:335–347
  20. Obert LA, Hoover EA: Early target cells in mucosal FIV infection. *J Virol* 2002, 76:6311–6322
  21. Billaud JN, Selway D, Yu N, Phillips TR: Replication rate of feline immunodeficiency virus in astrocytes is envelope dependent: implications for glutamate uptake. *Virology* 2000, 266:180–188
  22. Dow SW, Dreitz MJ, Hoover EA: Feline immunodeficiency virus neurotropism: evidence that astrocytes and microglia are the primary target cells. *Vet Immunol Immunopathol* 1992, 35:23–35
  23. Beebe AM, Faith TG, Sparger EE, Torten M, Pedersen NC, Dandekar S: Evaluation of in vivo and in vitro interactions of feline immunodeficiency virus and feline leukemia virus. *AIDS* 1994, 8:873–878
  24. Orandle MS, Papadi GP, Bubenik LJ, Dailey CI, Johnson CM: Selective thymocyte depletion and immunoglobulin coating in the thymus of cats infected with feline immunodeficiency virus. *AIDS Res Hum Retroviruses* 1997, 13:611–620
  25. Johnson CM, Papadi GP, Tompkins WA, Sellon RK, Orandle MS, Bellah JR, Bubenik LJ: Biphasic thymus response by kittens inoculated with feline immunodeficiency virus during fetal development. *Vet Pathol* 1998, 35:191–201
  26. Burkhard MJ, Obert LA, O'Neil LL, Diehl LJ, Hoover EA: Mucosal transmission of cell-associated and cell-free feline immunodeficiency virus. *AIDS Res Hum Retroviruses* 1997, 13:347–355
  27. Gunn-Moore DA, Pearson GR, Harbour DA, Whiting CV: Encephalitis associated with giant cells in a cat with naturally occurring feline immunodeficiency virus infection demonstrated by in situ hybridization. *Vet Pathol* 1996, 33:699–703
  28. Beebe AM, Dua N, Faith TG, Moore PF, Pedersen NC, Dandekar S: Primary stage of feline immunodeficiency virus infection: viral dissemination and cellular targets. *J Virol* 1994, 68:3080–3091
  29. Diehl LJ, Mathiason-DuBard CK, O'Neil LL, Obert LA, Hoover EA: Accelerated disease progression produced by feline immunodeficiency virus infection. *Keystone Symposia* 1995
  30. Diehl LJ, Mathiason-DuBard CK, O'Neil LL, Hoover EA: Longitudinal assessment of feline immunodeficiency virus kinetics in plasma by use of a quantitative competitive reverse transcriptase PCR. *J Virol* 1995, 69:2328–2332
  31. Burkhard MJ, Obert L, Diehl L, Hoover E: Mucosal transmission of cell-associated vs cell-free feline immunodeficiency virus. *Vet Pathol* 1995, 32:A593
  32. Diehl LJ, Mathiason-DuBard CK, O'Neil LL, Obert LA, Hoover EA: Induction of accelerated feline immunodeficiency virus disease by acute phase virus passage. *J Virol* 1995, 69:6149–6157
  33. Obert LA, Hoover EA: Feline immunodeficiency virus clade C mucosal transmission and disease courses. *AIDS Res Hum Retroviruses* 2000, 16:677–688
  34. Sodora DL, Shpaer EG, Kitchell BE, Dow SW, Hoover EA, Mullins JL: Identification of three feline immunodeficiency virus (FIV) env gene subtypes and comparison of the FIV and human immunodeficiency virus type 1 evolutionary patterns. *J Virol* 1994, 68:2230–2238
  35. O'Neil LL, Burkhard MJ, Diehl LJ, Hoover EA: Vertical transmission of feline immunodeficiency virus. *AIDS Res Hum Retroviruses* 1995, 11:171–182
  36. Diehl LJ, Mathiason-Dubard CK, O'Neil LL, Obert LA, Hoover EA: Induction of accelerated feline immunodeficiency virus disease by acute-phase virus passage. *J Virol* 1995, 69:6149–6157
  37. Dreitz MJ, Dow SW, Fiscus SA, Hoover EA: Development of monoclonal antibodies and capture immunoassays for feline immunodeficiency virus. *Am J Vet Res* 1995, 56:764–768
  38. Yamate J, Yoshida H, Tsukamoto Y, Ide M, Kuwamura M, Ohashi F, Miyamoto T, Kotani T, Sakuma S, Takeya M: Distribution of cells immunopositive for AM-3K, a novel monoclonal antibody recognizing human macrophages, in normal and diseased tissues of dogs, cats, horses, cattle, pigs, and rabbits. *Vet Pathol* 2000, 37:168–176
  39. Zeng L, Takeya M, Ling X, Nagasaki A, Takahashi K: Interspecies reactivities of anti-human macrophage monoclonal antibodies to various animal species. *J Histochem Cytochem* 1996, 44:845–853
  40. Zeng L, Takeya M, Takahashi K: AM-3K, a novel monoclonal antibody specific for tissue macrophages and its application to pathological investigation. *J Pathol* 1996, 178:207–214
  41. Groshek PM, Dean GA, Hoover EA: Monoclonal antibodies identifying feline hemopoietic cell lineages. *Comp Haematol Int* 1995, 4:181–191
  42. Podell M, Oglesbee M, Mathes L, Krakowka S, Olmstead R, Lafrado L: AIDS-associated encephalopathy with exoclonal feline immunodeficiency virus infection. *J Acquir Immune Defic Syndr* 1993, 6:758–771
  43. Carbone A, Manconi R, Poletti A, Volpe R: Significance of S-100 protein immunostaining in the immunohistological analysis of normal and neoplastic lymphoid tissues—an appraisal. *Int J Biol Markers* 1986, 1:57–66
  44. Gillespie JW, Best CJ, Bichsel VE, Cole KA, Greenhut SF, Hewitt SM, Ahram M, Gathright YB, Merino MJ, Strausberg RL, Epstein JI, Hamilton SR, Gannot G, Baibakova GV, Calvert VS, Flaig MJ, Chuaqui RF, Herring JC, Pfeifer J, Petricoin EF, Linehan WM, Duray PH, Bova GS,



- Emmert-Buck MR: Evaluation of non-formalin tissue fixation for molecular profiling studies. *Am J Pathol* 2002, 160:449–457
45. Veazey RS, DeMaria M, Chalifoux LV, Shvets DE, Pauley DR, Knight HL, Rosenzweig M, Johnson RP, Desrosiers RC, Lackner AA: Gastrointestinal tract as a major site of CD4+ T cell depletion and viral replication in SIV infection. *Science* 1998, 280:427–431
  46. Belyakov IM, Hel Z, Kelsall B, Kuznetsov VA, Ahlers JD, Nacsa J, Watkins DI, Allen TM, Sette A, Altman J, Woodward R, Markham PD, Clements JD, Franchini G, Strober W, Berzofsky JA: Mucosal AIDS vaccine reduces disease and viral load in gut reservoir and blood after mucosal infection of macaques. *Nat Med* 2001, 7:1320–1326
  47. Williams KC, Corey S, Westmoreland SV, Pauley D, Knight H, deBaker C, Alvarez X, Lackner AA: Perivascular macrophages are the primary cell type productively infected by simian immunodeficiency virus in the brains of macaques: implications for the neuropathogenesis of AIDS. *J Exp Med* 2001, 193:905–915
  48. Liang Y, Hudson LC, Levy JK, Ritchey JW, Tompkins WA, Tompkins MB: T cells overexpressing interferon-gamma and interleukin-10 are found in both the thymus and secondary lymphoid tissues of feline immunodeficiency virus-infected cats. *J Infect Dis* 2000, 181:564–575
  49. Li SL, Kaaya EE, Ordonez C, Ekman M, Feichtinger H, Putkonen P, Bottiger D, Biberfeld G, Biberfeld P: Thymic immunopathology and progression of SIVsm infection in cynomolgus monkeys. *J Acquir Immune Defic Syndr Hum Retrovirol* 1995, 9:1–10
  50. Diehl LJ, Mathiason-DuBard CK, O'Neil LL, Hoover EA: Plasma viral RNA load predicts disease progression in an accelerated feline immunodeficiency virus model. *J Virol* 1996, 70:2503–2507
  51. O'Neil LL, Burkhard MJ, Hoover EA: Frequent perinatal transmission of feline immunodeficiency virus by chronically infected cats. *J Virol* 1996, 70:2894–2901
  52. Bannert N, Schenten D, Craig S, Sodroski J: The level of CD4 expression limits infection of primary rhesus monkey macrophages by a T-tropic simian immunodeficiency virus and macrophagetropic human immunodeficiency viruses. *J Virol* 2000, 74:10984–10993
  53. Clapham PR, Reeves JD, Simmons G, DeJucq N, Hibbitts S, McKnight A: HIV coreceptors, cell tropism and inhibition by chemokine receptor ligands. *Mol Membr Biol* 1999, 16:49–55
  54. Haase AT: Population biology of HIV-1 infection: viral and CD4+ T cell demographics and dynamics in lymphatic tissues. *Annu Rev Immunol* 1999, 17:625–656
  55. Stahl-Hennig C, Steinman RM, Tenner-Racz K, Pope M, Stolte N, Matz-Rensing K, Grobshupff G, Raschdorff B, Hunsmann G, Racz P: Rapid infection of oral mucosal-associated lymphoid tissue with simian immunodeficiency virus. *Science* 1999, 285:1261–1265
  56. Meng G, Sellers MT, Mosteller-Barnum M, Rogers TS, Shaw GM, Smith PD: Lamina propria lymphocytes, not macrophages, express CCR5 and CXCR4 and are the likely target cell for human immunodeficiency virus type 1 in the intestinal mucosa. *J Infect Dis* 2000, 182:785–791
  57. Joag SV, Adany I, Li Z, Foresman L, Pinson DM, Wang C, Stephens EB, Raghavan R, Narayan O: Animal model of mucosally transmitted human immunodeficiency virus type 1 disease: intravaginal and oral deposition of simian/human immunodeficiency virus in macaques results in systemic infection, elimination of CD4+ T cells, and AIDS. *J Virol* 1997, 71:4016–4023
  58. Hu J, Gardner MB, Miller CJ: Simian immunodeficiency virus rapidly penetrates the cervicovaginal mucosa after intravaginal inoculation and infects intraepithelial dendritic cells. *J Virol* 2000, 74:6087–6095
  59. Zhang Z, Schuler T, Zupancic M, Wietgreffe S, Staskus KA, Reimann KA, Reinhart TA, Rogan M, Cavert W, Miller CJ, Veazey RS, Notermans D, Little S, Danner SA, Richman DD, Havlir D, Wong J, Jordan HL, Schacker TW, Racz P, Tenner-Racz K, Letvin NL, Wolinsky S, Haase AT: Sexual transmission and propagation of SIV and HIV in resting and activated CD4+ T cells [published erratum appears in *Science* 1999, 286:2273]. *Science* 1999, 286:1353–1357